



Comparative Studies of Photophysicochemical Properties of Non-Peripherally Anisole/Thioanisole-Tetrasubstituted Gallium(III) Phthalocyanines Containing Oxygen/ Sulfur Bridge

Armağan Günsel*

Sakarya University, Department of Chemistry, TR54187 Serdivan, Sakarya, Turkey

Abstract: In this work, we have presented the synthesis and characterization of gallium(III) phthalocyanines (**4-6**) which are non-peripherally tetra-substituted with anisole or thioanisole functional groups containing oxygen or sulfur bridge. Confirmation of the phthalocyanine structures performed with the cooperation of elemental analysis, FTIR, ¹H-NMR, UV-Vis and MALDI-MS spectral data. Also, we have investigated and discussed the effects of non-peripherally tetra-substitution with different functional groups on the photochemical and photophysical properties (singlet oxygen quantum yield, photodegradation quantum yield, fluorescence quantum yield and fluorescent behavior). In every substituent, we obtained very similar singlet oxygen quantum yields as 0.64 for (**4**), 0.56 for (**5**) and 0.65 for (**6**) suggesting their potential as photosensitizer in PDT treatment.

Keywords: Phthalocyanine, anisole, thioanisole, gallium, photochemistry.

Submitted: November 24, 2017. **Accepted:** December 28, 2017.

Cite this: Günsel A. Comparative Studies of Photophysicochemical Properties of Non-Peripherally Anisole/Thioanisole-Tetrasubstituted Gallium(III) Phthalocyanines Containing Oxygen/ Sulfur Bridge. JOTCSA. 2018;5(1):269-89.

DOI: <http://dx.doi.org/10.18596/jotcsa.357551>

Corresponding Author. E-mail: agunsel@sakarya.edu.tr. **Tel.:** +90 264 295 6070/

INTRODUCTION

Phthalocyanines (Pcs) are highly conjugated macrocycles which have the ability to form complexes with many different metals. Because of having their chemical, photophysical, and photochemical properties as well as their stability (1), Pcs have been used for development of photosensitizers in photodynamic therapy (2,3), dye-sensitized solar cells (4), organic semiconductors (5), electrochromic displays (6), non-linear optical materials (7), liquid crystals (8), chemical sensors (9), and electrochromic agents (10).

Because of their low solubility, unsubstituted phthalocyanines tend to be in the aggregated form in common organic solvents but they can become soluble in many solvents by attaching some functional groups such as methoxy or methylthio groups at peripheral or non-peripheral positions of Pcs. These kind of groups have extensively been used in both medical and industrial purposes like antiallergenic, antiarterogenic, antiinflammatory, antimicrobial, antioxidant, antithrombotic, cardioprotective, and vasodilatory effects. Non-peripheral substitution causes red-shift in the Q-band, suggesting optimal transparency into tissue in PDT(11–16).

The strong absorption of phthalocyanines in the region of 650-680 nm and high efficiency in producing reactive oxygen species (ROS), *e.g.* singlet oxygen ($^1\text{O}_2$), causing destruction of cancer cells, led to the development of photodynamic cancer therapy (PDT) over the last century. The variety of metal ion that is inserted to the inner core of phthalocyanines strongly influences the ROS production. Especially, phthalocyanines containing diamagnetic ions (Zn^{2+} , In^{3+} , Ga^{3+} *etc.*) exhibit sufficient photophysical and photochemical properties (triplet quantum yield, lifetime and singlet oxygen generation) because of high ROS yields for PDT(17,18).

In this paper, we have firstly presented the synthesis and characterization of anisole or thioanisole tetra-substituted gallium(III) phthalocyanines (**4-6**) containing oxygen or sulfur bridge at non-peripheral positions, which show good solubility in common organic solvents. Finally, the photochemical and photophysical properties (singlet oxygen quantum yield, photodegradation quantum yield, fluorescent quantum yields and fluorescent behavior) of the synthesized gallium(III) phthalocyanines (**4-6**) in DMSO were investigated to compare the effect of different substituent, which is very important for biological cell studies on PDT.

EXPERIMENTAL

Materials and Methods

3-(4-Methoxy-phenoxy)phthalonitrile (**1**), 3-(4-(methylthio)phenoxy)phthalonitrile (**2**), 3-(4-(methylthio)phenylthio)phthalonitrile (**3**) and 1(4), 8(11), 15(18), 22(25)-tetrakis (3-(4-(methylthio)phenylthio))phthalocyaninatogallium(III) chloride (**6**) were prepared according to

the procedures in literature (4,19,20). Some chemicals such as dimethyl sulfoxide (DMSO) and GaCl₃ were acquired from Merck and Alfa Aesar and used as received. UV-Vis spectra were acquired in a quartz cuvette on an Agilent Model 8453 diode array spectrophotometer. Perkin-Elmer Spectrum Two FT-IR spectrometer was used to acquire FT-IR spectra. All the products were purified by column chromatography on silica gel (Merck grade 60) from Aldrich. All reactions were achieved under a dry N₂ atmosphere. A Bruker 300 spectrometer was used to record ¹H NMR spectra. Mass spectra (MS) were analyzed by MALDI SYNAPT G2-Si Mass Spectrometer. Fluorescence spectra were measured using a Varian Eclipse spectrofluorometer using 1-cm path length cuvettes at room temperature. Photo-irradiations for singlet oxygen determination were measured using a General Electric quartz line lamp (300 W). A 600 nm glass cut off filter (Schott) and a water filter were used to filter off ultraviolet and infrared radiations, respectively. An interference filter (Intor, 700nm with a bandwidth of 40nm) was additionally placed in the light path before the sample. Light intensities were measured with a POWER MAX 5100 (Mol electron detector incorporated) power meter.

Synthesis

General procedure for the synthesis of gallium phthalocyanines (GaPcs): Reaction: A mixture of **(1)** or **(2)** (0.100 g, ~0.39 mmol), GaCl₃ (0.018 g, 0.10 mmol) and a catalytic amount of DBU (1,8-diazabicyclo[5.4.0]undec-7-ene) in n-hexanol (2 cm³) was refluxed at 160 °C in a sealed glass tube for 10 hours under N₂ atmosphere. After cooling to room temperature, the green crude product was cooled and precipitated by adding n-hexane and filtered. *Purification:* After being washed with methanol, it was purified by silica gel column chromatography (CH₂Cl₂/ethanol 50/2, v/v) and finally dried *in vacuo* at 100 °C. Solubility: Highly soluble in THF, CH₂Cl₂, DMSO, and DMF.

1(4), 8(11), 15(18), 22(25)-Tetrakis (3-(4-methoxy-phenoxy)phthalocyaninato gallium(III) chloride(4)

The product was soluble in CHCl₃, CH₂Cl₂, THF, DMF, and DMSO. Yield of **(4)**: 0.036 g (33%). Anal. calcd. For (%) C₆₀H₄₀ClGa₈N₈O₈ (1106.18 g/mol): C, 65.15; H, 3.64; N, 10.13; Found: C, 64.49; H, 3.80; N, 9.58. FT-IR (u_{max}/cm⁻¹): 3062 (Ar-H), 2948, 2914, 2855 (Aliph. C-H), 1722, 1625 (C=C), 1574, 1517, 1480, 1428, 1315, 1220, 1105, 892, 741. UV-Vis (DMSO): λ_{max}/nm (log ε): 713 (4.65), 641 (3.98), 322 (4.45). ¹H-NMR (300 MHz, CDCl₃) δ ppm: 7.84-7.64 (m, 12H, Pc-H), 7.44-7.10 (m, 16H, Ar-H), 2.12 (s, 12H CH₃-OAr). MS (MALDI-TOF, 2,5-dihydroxybenzoic acid as matrix): m/z 1071.68 [M-Cl+H]⁺.

1(4),8(11),15(18), 22(25)-Tetrakis (3-(4-(methylthio)phenoxy)phthalocyaninato gallium(III) chloride(5)

The product was soluble in CHCl₃, CH₂Cl₂, THF, DMF, and DMSO. Yield of **(5)**: 0.033 g (30%). Anal. calcd. For (%)C₆₀H₄₀ClGa₈O₄S₄ (1170.45 g/mol): C, 61.57; H, 3.44; N, 9.57; Found: C,

60.55; H, 3.41; N, 9.71. FT-IR ($\nu_{\max}/\text{cm}^{-1}$): 3049 (Ar-H), 2961, 2862 (Aliph. C-H), 1733, 1631 (C=C), 1560, 1521, 1447, 1431, 1314, 1221, 1105, 841, 702, 612. UV-Vis (DMSO): λ_{\max}/nm ($\log \epsilon$): 712 (4.65), 639 (3.96), 358 (4.15). $^1\text{H-NMR}$ (300 MHz, CDCl_3) δ ppm: 7.79-7.55 (m, 12H, Pc-H), 7.38-7.14 (m, 16H, Ar-H), 2.20 (s, 12H CH_3 -SAr). MS (MALDI-TOF, 2,5-dihydroxybenzoic acid as matrix): m/z 1135.88 $[\text{M-Cl+H}]^+$.

Photophysical and Photochemical Studies

Fluorescence quantum yields: Fluorescence quantum yields (Φ_F) were determined by the comparative method **(Eq. 1)(21)**,

$$\Phi_F = \Phi_{F(\text{Std})} \times \frac{F \cdot A_{\text{Std}} \cdot n^2}{F_{\text{Std}} \cdot A \cdot n_{\text{Std}}^2} \quad \text{(Eq. 1)}$$

where F and F_{Std} are the areas under the fluorescent emission curves of the samples and the standard, respectively. A and A_{Std} are the respective absorbances of the samples and standard (Unsubstituted ZnPc) at the excitation wavelengths, respectively. n^2 and $n_{(\text{Std})}^2$ are the refractive indices of solvents used for the sample and standard, respectively. Unsubstituted ZnPc in DMSO ($\Phi_F = 0.20$)(22) was used as the standard. Both the samples and standard were excited at the same wavelength. The absorbance of the solutions at the excitation wavelength ranged between 0.04 and 0.05.

Singlet oxygen quantum yields: Singlet oxygen quantum yield (Φ_Δ) determinations were carried out by using the experimental set-up described in the literature(23). Quantum yields of singlet oxygen photogeneration were determined in air (no oxygen bubbled) using the relative method with ZnPc as reference and DPBF (1,3-diphenylisobenzofuran) as the chemical quencher for singlet oxygen, using formula **(Eq. 2)**,

$$\Phi_\Delta = \Phi_\Delta^{\text{Std}} \times \frac{R \cdot I_{\text{abs}}^{\text{Std}}}{R_{\text{Std}} \cdot I_{\text{abs}}} \quad \text{(Eq. 2)}$$

where Φ_Δ^{Std} is the singlet oxygen quantum yield for ZnPc standard ($\Phi_\Delta^{\text{Std}} = 0.67$ in DMSO(24)). R and R_{Std} are the DPBF photobleaching rates in the presence of the respective samples and standard, respectively. I_{abs} and $I_{\text{abs}}^{\text{Std}}$ are the rates of light absorption by the samples and standard, respectively. To avoid chain reactions induced by DPBF in the presence of singlet oxygen (24,25), the concentration of quencher (DPBF) was lowered to $\sim 3 \times 10^{-5} \text{ mol dm}^{-3}$. Solutions of the sensitizer (containing DPBF) were prepared in the dark and irradiated in the Q band region using the set up described above. DPBF degradation was monitored at 417 nm. The light intensity of $7.05 \times 10^{15} \text{ photons s}^{-1} \text{ cm}^{-2}$ was used for Φ_Δ determinations.

Photodegradation quantum yields: Photodegradation quantum yield (Φ_d) determinations were carried out using the experimental set-up described in literature (26). Photodegradation quantum yields were determined using formula **(Eq.3)**,

$$\Phi_d = \frac{(C_0 - C_t) \cdot V \cdot N_A}{I_{\text{abs}} \cdot S \cdot t} \quad \text{(Eq. 3)}$$

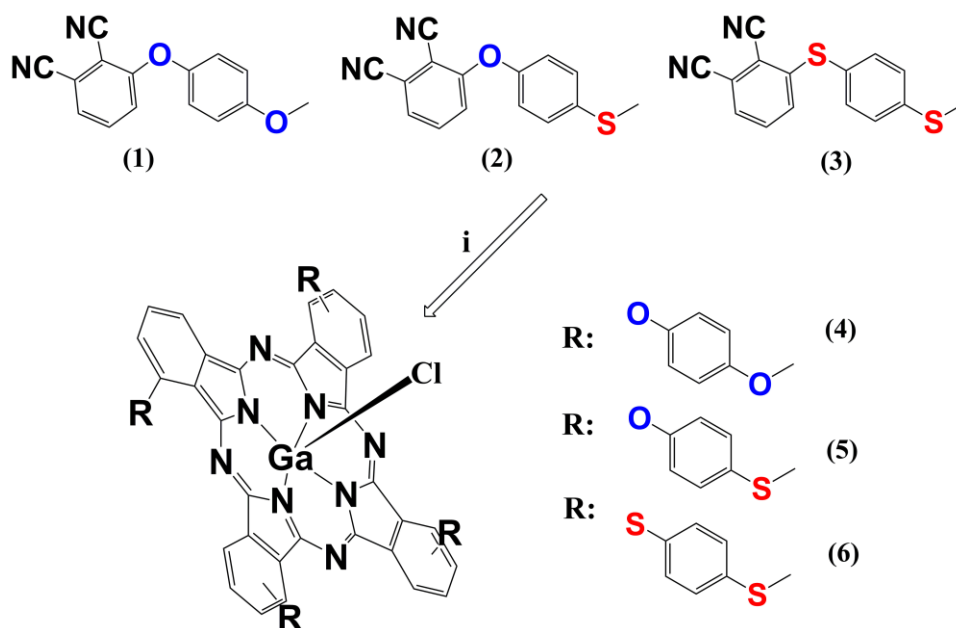
where " C_0 " and " C_t " are the sample concentrations before and after irradiation respectively, " V " is the reaction volume, " N_A " is the Avogadro's constant, " S " is the irradiated cell area, " t " is the irradiation time, " I_{abs} " is the overlap integral of the radiation source light intensity and the absorption of the samples. A light intensity of 2.38×10^{16} photons $\text{s}^{-1} \text{cm}^{-2}$ was employed for Φ_d determinations.

RESULTS AND DISCUSSION

Synthesis and Spectroscopic Characterization

The characterization of all synthesized compounds was carried out with the aid of some spectroscopic methods such as FT-IR, $^1\text{H-NMR}$ and UV-Vis spectroscopic methods, elemental analysis and mass spectra which gave very satisfactory results.

Non-peripherally tetrasubstituted phthalocyanines **(4)** and **(5)** were prepared by cyclotetramerization of 3-(4-methoxy-phenoxy)phthalonitrile **(1)** or 3-(4-(methylthio)phenoxy)phthalonitrile **(2)**. The preparation of phthalocyanines **(4)** and **(5)** from the aromatic dinitriles were carried out under the same reaction conditions by treatment of phthalonitriles **(1)** or **(2)** with GaCl_3 in dry n-hexanol and 1,8-diazabicyclo[5.4.0]undec-7-ene (DBU) at 160°C , for 10 h **(Scheme 1)**.



Scheme 1. General procedure for the synthesis of gallium phthalocyanines (GaPcs) **(4-6)**, **i**: GaCl₃, 160 °C, for 10h, n-hexanol, and DBU.

The UV-Vis spectra of phthalocyanines **(4)** and **(5)** were recorded in DMSO. The UV-Vis spectra of phthalocyanines **(4)** and **(5)** were obtained as a single band of high intensity at 713 nm (Q) for **(4)**, 712 nm (Q) for **(5)**, respectively that are typical of phthalocyanine complexes. Phthalocyanines indicate characteristic B-band in addition to Q band absorption, in the UV region at 322 nm for **(4)** and 358 nm for **(5)** respectively.

In the FT-IR-spectra, after conversion into phthalocyanines **(4)** and **(5)**, the characteristic -C≡N peaks for **(1)** and **(2)** were not observed for **(4)** and **(5)** as expected and thus, proved the formation of these compounds **(4)** and **(5)** from the corresponding dinitriles **(1)** and **(2)**.

The synthesized phthalocyanine complexes **(4)** and **(5)** are very similar to each other and showed characteristic vibrations which belong to the ether groups at ~1220 cm⁻¹, the aromatic CH stretching at ca. 3049-3062 cm⁻¹ and the aliphatic CH stretching at ca. 2855-2961 cm⁻¹.

In ¹H NMR spectra of the phthalocyanines **(4)** and **(5)**, the obtained signals for the phthalocyanines **(4)** and **(5)** are quite broader compared to the signals of the starting compounds **(1)** and **(2)**. The protons were observed between 7.84-7.55 ppm on aromatic structure for Pc-ring, and between 7.44-7.10 ppm aromatic structure for functional groups. Additionally, the protons were observed at around 2.12 and 2.20 ppm respectively as singlet for the O-CH₃ and S-CH₃ groups.

In the MALDI-TOF mass spectra, the observation of the characteristic molecular ion peaks at m/z 1071.68 $[M-Cl+H]^+$ for **(4)** (**Figure 1.A**) and at m/z 1135.88 $[M-Cl+H]^+$ for **(5)** (**Figure 1.B**) confirmed the proposed structure.

Last, elemental analysis of both complexes gave satisfactory results corresponding to all synthesized compounds.

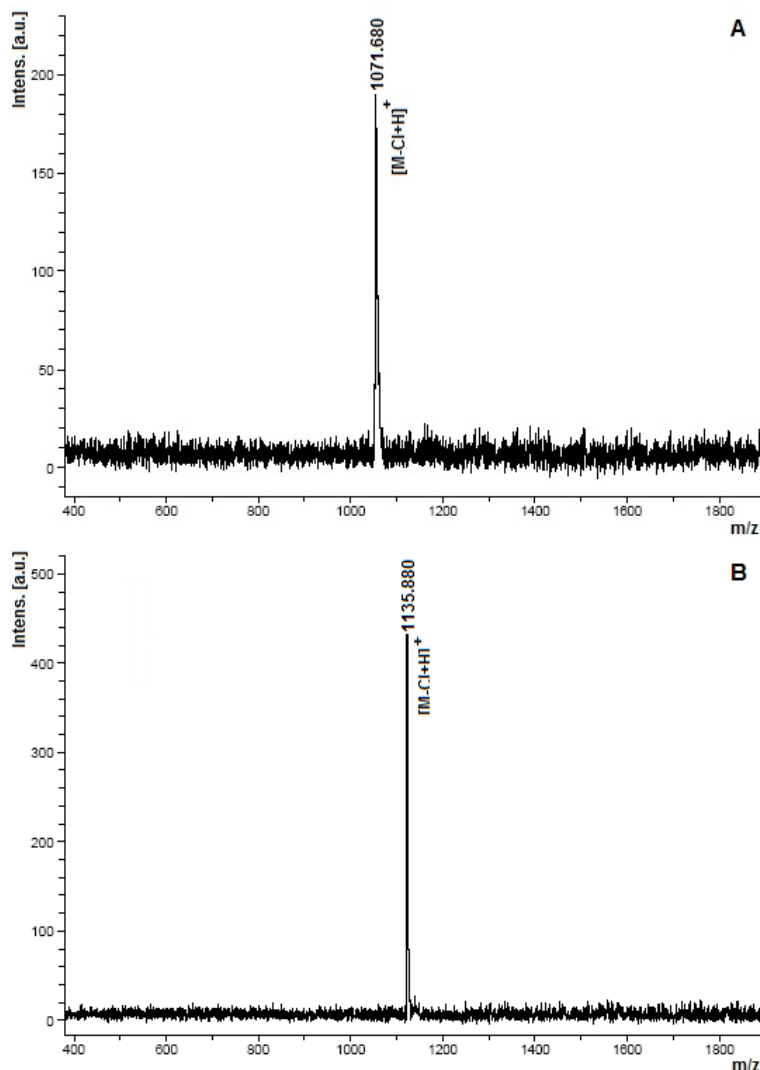


Figure 1: MALDI-TOF MS spectra of compound **(4, A)** and **(5, B)**.

Aggregation studies

An intense and sharp Q-band was observed in the absorption spectra of the phthalocyanines **(4-6)** in DMSO, exhibiting the evidence of the formation of non-aggregated forms. Dilution studies in DMSO were done to test the aggregation of the phthalocyanines **(4-6)** (**Figure 2.(A-C)** shows the spectra of the synthesized phthalocyanines **(4-6)** in DMSO at various concentrations). The increasing of the Pc concentration led to an increase in the intensity of absorption of the Q band. No new band formation was observed because of the aggregated forms(27,28). From these results, we can conclude that the phthalocyanines **(4-6)** did not aggregate in the solvent of

DMSO and the Lambert-Beer law was obeyed for the synthesized phthalocyanines at the concentration ranging from 3.59×10^{-5} to 2.24×10^{-6} M for **(4)**, 3.52×10^{-5} to 2.20×10^{-6} M for **(5)** and 3.65×10^{-5} to 2.25×10^{-6} M for **(6)** respectively.

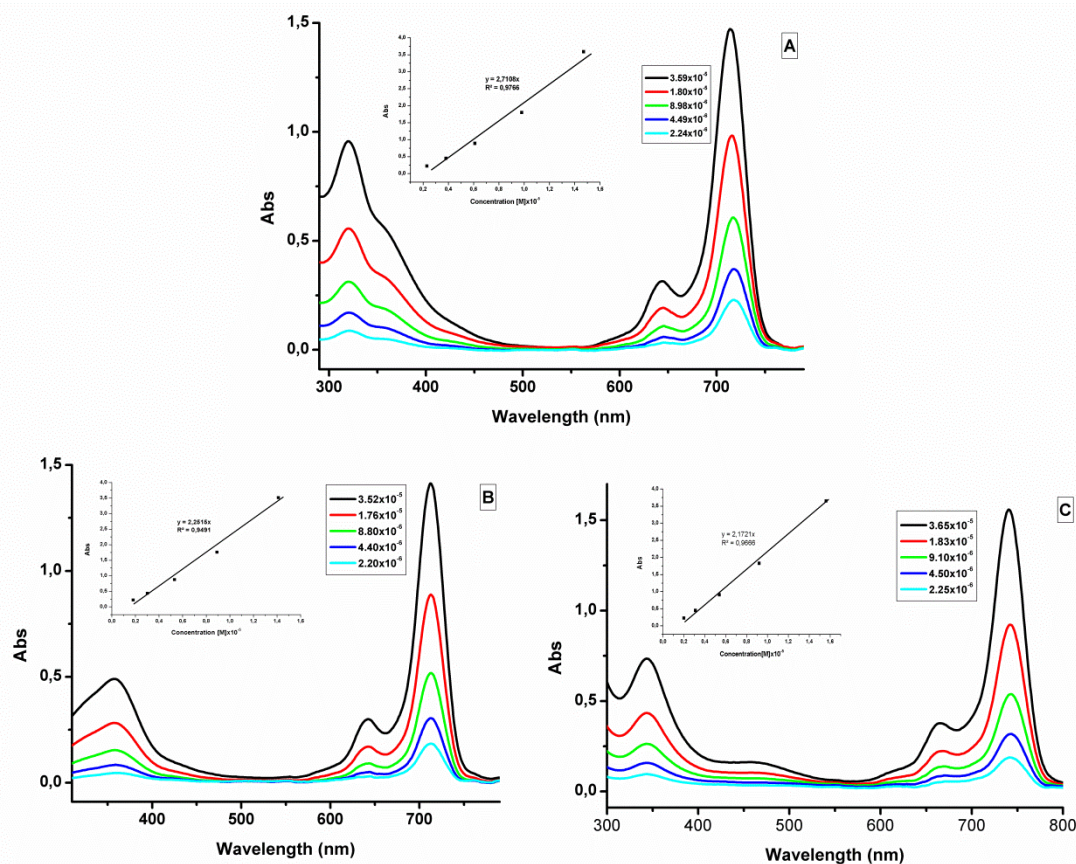


Figure 2: UV-Vis absorption spectra of the phthalocyanines **(4:A)**, **(5:B)** and **(6:C)** in DMSO at different concentrations.

Photophysical and photochemical studies

Fluorescence quantum yields: The measurement of fluorescent quantum yields was determined in DMSO. The comparison of spectra was also carried out under the same conditions (Figures 3 and 4). While the complexes **(4)** and **(5)** have typical fluorescent behavior, the complex **(6)** shows that the fluorescence excitation spectrum is blue-shifted by about 10 nm relative to that of the absorption spectrum, suggesting a change in geometry upon excitation (20). The quantum yield results are; for **(4)** in DMSO 0.138, for **(5)** in DMSO 0.101 and for **(6)** in DMSO 0.050. The yields of the complexes **(4)** and **(5)** are almost similar but the complex **(6)** is lower fluorescent quantum yields than the complexes **(4)** and **(5)**. These compounds have lower fluorescent quantum yields than standard GaPc ($\Phi_F = 0.30$ in DMSO).

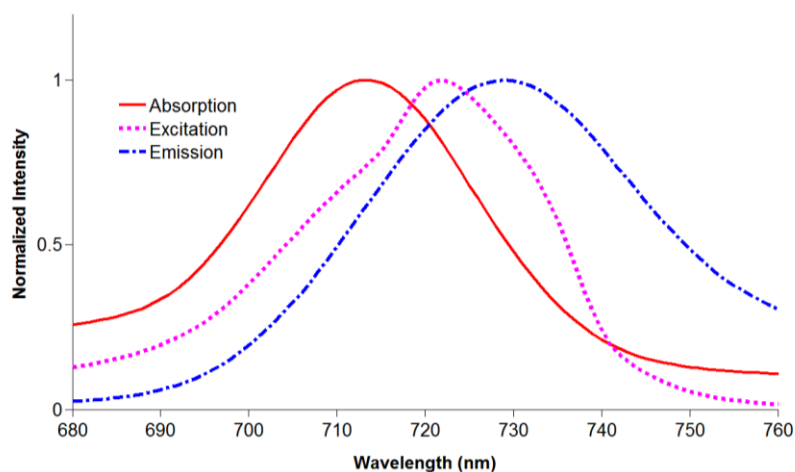


Figure 3: Absorption (713 nm), excitation (721 nm) and emission (729 nm) spectra of **(4)** in DMSO.

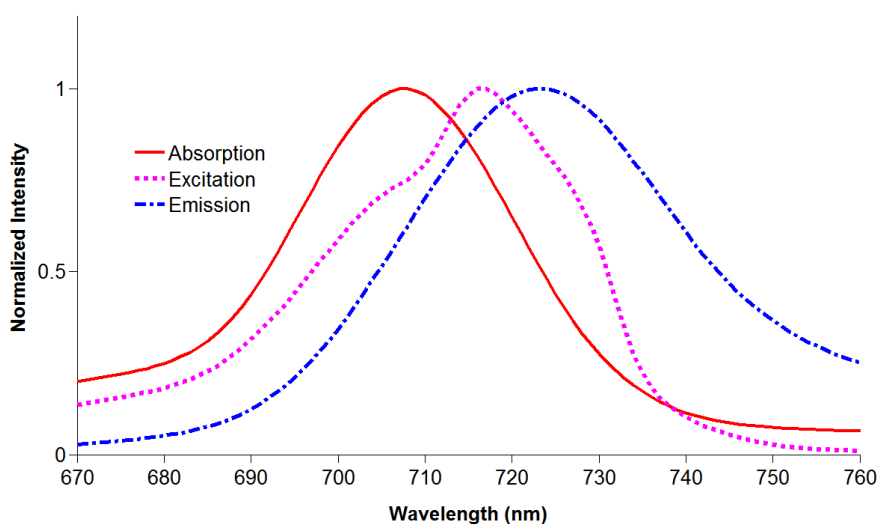


Figure 4: Absorption (708 nm), excitation (717 nm) and emission (723 nm) spectra of **(5)** in DMSO.

Singlet oxygen quantum yields: The singlet oxygen quantum yields in the presence of different substituents were determined in DMSO by following the chemical method based on the chemical quenching of DPBF (1,3-diphenylisobenzofuran) in order to investigate the effect of substituents (Figures 5,6, and 7). In every substituent, the complex showed similar quantum yields. As shown in Table 1, the highest quantum yield Φ_{Δ} (0.65) is for complex **(6)**, followed by complex **(4)** Φ_{Δ} (0.64) and complex **(5)** Φ_{Δ} (0.56). The yields of singlet oxygen for all synthesized complexes have very high values when compared to unsubstituted GaPc.

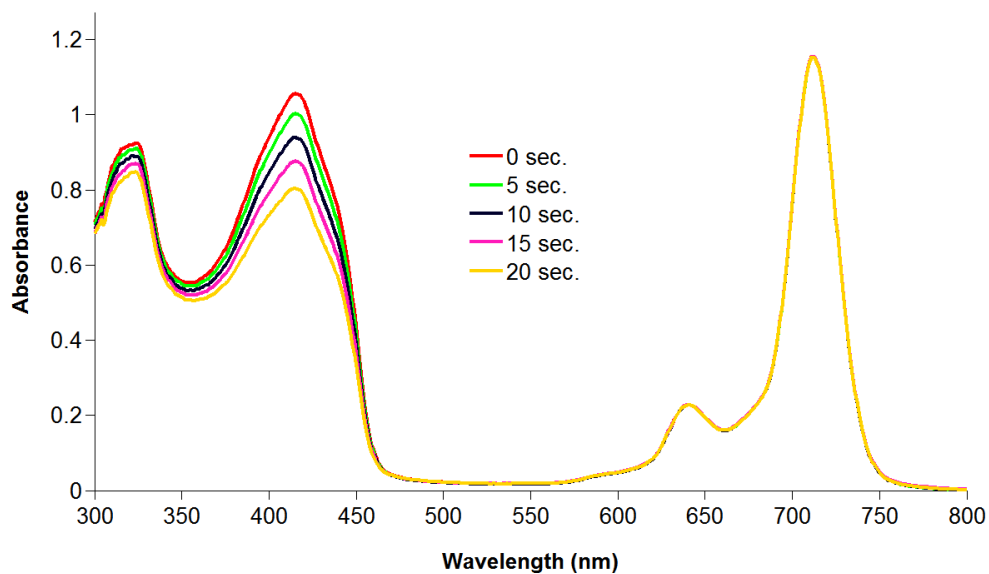


Figure 5: A typical spectrum for the determination of singlet oxygen quantum yield of **(4)** in DMSO.

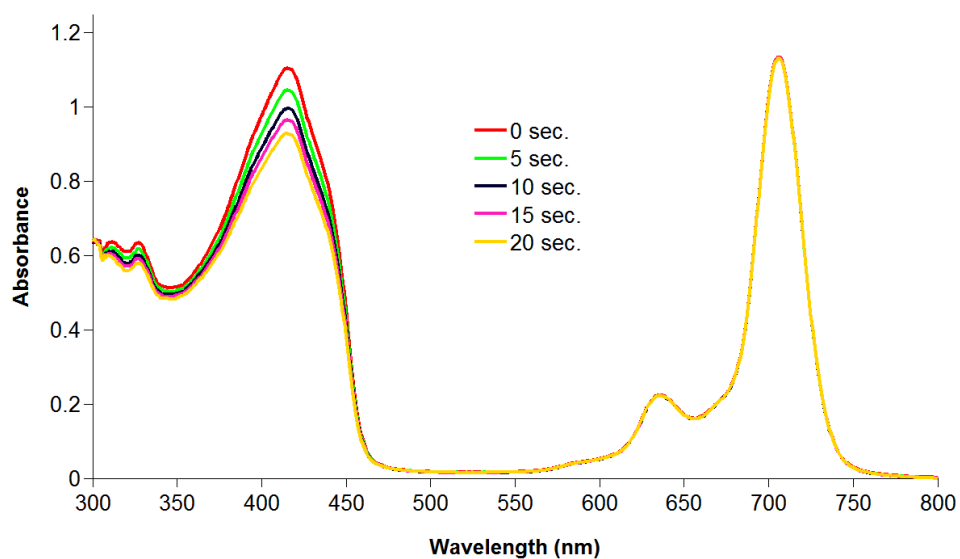


Figure 6: A typical spectrum for the determination of singlet oxygen quantum yield of **(5)** in DMSO.

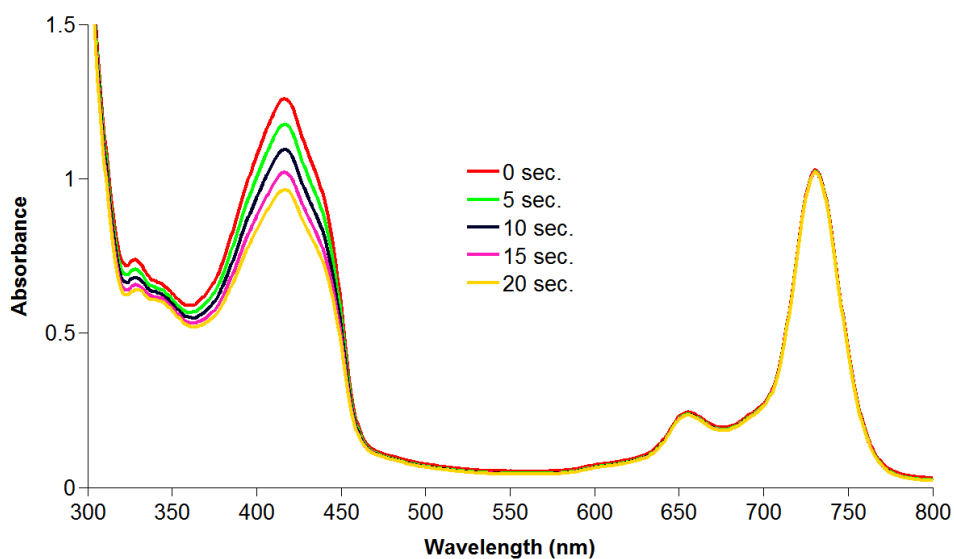


Figure 7: A typical spectrum for the determination of singlet oxygen quantum yield of **(6)** in DMSO.

Photodegradation quantum yields: The quantum yield values of the order 10^{-4} were given Table 1 and the spectral changes observed for the complexes are shown in (Figures 8,9, and 10). Unsubstituted GaPc complexes as a reference is less stable than these complexes. Photodegradation quantum yield (Φ_d) value of complex **(5)** in DMSO ($\Phi_d: 2,9 \times 10^{-4}$) is less stable as compared to the other complexes. But in generally, it can be said that all the complexes are resistant to photochemical degradation.

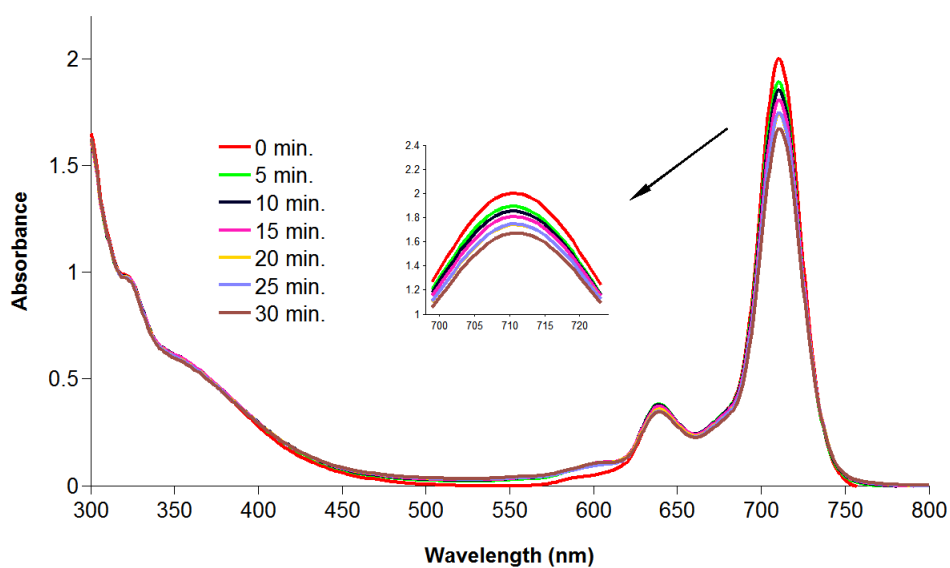


Figure 8: A typical spectrum for the determination of photodegradation of **(4)** in DMSO.

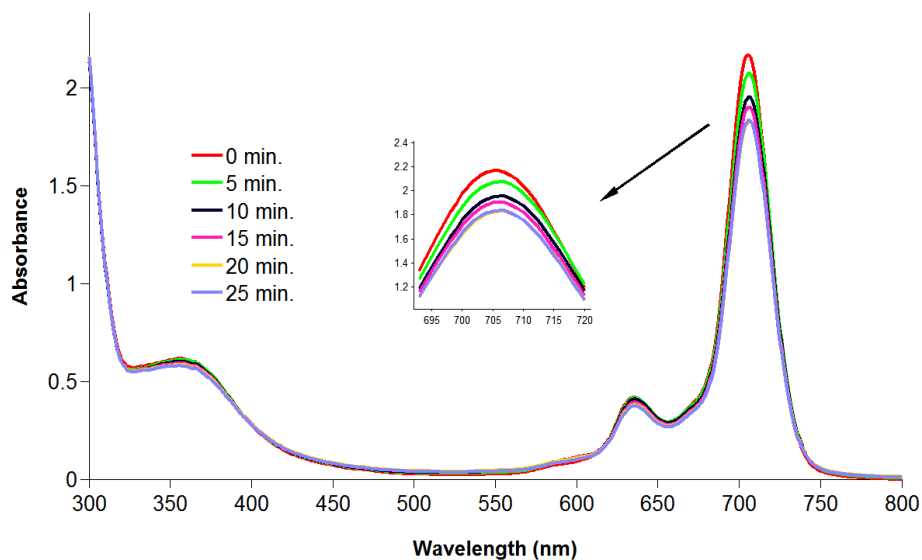


Figure 9: A typical spectrum for the determination of photodegradation of **(5)** in DMSO.

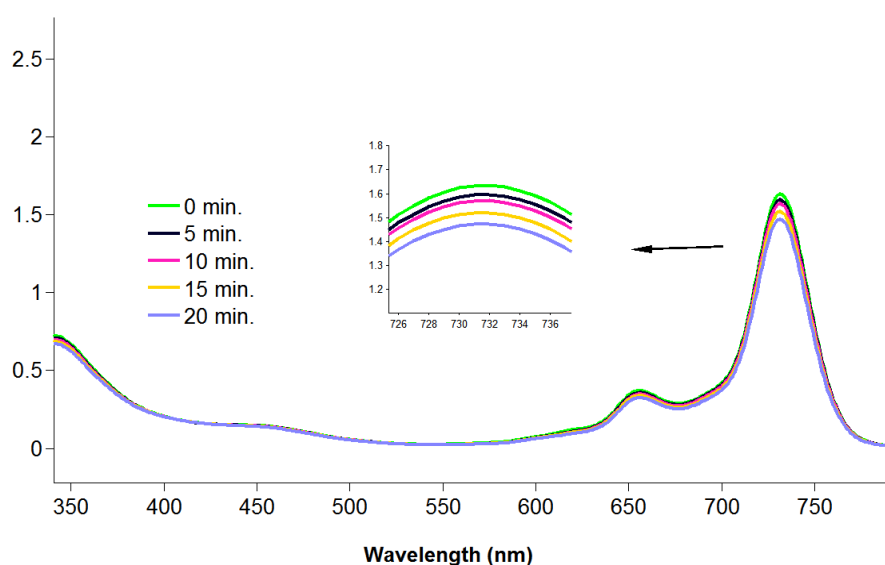


Figure 10: A typical spectrum for the determination of photodegradation of **(6)** in DMSO.

Table 1: Photophysical and photochemical properties of the complexes in DMSO.

Complex	Q band, λ_{max} , (nm)	Excitation, (nm)	Emission, (nm)	Φ_F	$\Phi_d (10^{-4})$	Φ_Δ	Stokes shift, Δ_{stokes} , (nm)
(4)	713	721	729	0.138	15	0.64	16
(5)	708	717	723	0.101	2.9	0.56	15
(6)	742	732	744	0.050	40	0.65	2
GaPc^a	-	-	-	0.300	0.09	0.41	-

^a Data from (29).

CONCLUSION

In this paper, we have synthesized and characterized anisole or thioanisole tetra-substituted gallium(III) phthalocyanines (**4-6**) containing oxygen or sulfur bridge at the non-peripheral positions and then investigated and discussed the effects of different functional groups on the photochemical and photophysical properties. In every substituent, the complex exhibited similar quantum yield. The highest quantum yield Φ_{Δ} (0.65) is for complex (**6**), and then it is followed by complex (**4**) Φ_{Δ} (0.64) and complex (**5**) Φ_{Δ} (0.56).

Conflict of interest: The authors declare that they have no conflict of interest.

REFERENCES

1. McKeown NB. Phthalocyanine materials: synthesis, structure, and function. Cambridge, U.K.; New York: Cambridge University Press; 1998.
2. Güzel E, Günsel A, Bilgiçli AT, Atmaca GY, Erdogmus A, Yarasir MN. Synthesis and photophysicochemical properties of novel thiadiazole-substituted zinc (II), gallium (III) and silicon (IV) phthalocyanines for photodynamic therapy. *Inorganica Chim Acta*. 2017;467:169-76.
3. Günsel A, Güzel E, Bilgiçli AT, Atmaca GY, Erdogmus A, Yarasir MN. Synthesis and investigation of photophysicochemical properties of novel ketone-substituted gallium (III) and indium (III) phthalocyanines with high singlet oxygen yield for photodynamic therapy. *J Luminescence*. 2017;192:888-92.
4. Günsel A, Güzel E, Bilgiçli AT, Şişman İ, Yarasir MN. Synthesis of non-peripheral thioanisole-substituted phthalocyanines: Photophysical, electrochemical, photovoltaic, and sensing properties. *J Photochem. Photobiol. A*. 2017;348(Supplement C):57-67.
5. Günsel A, Kandaz M, Yakuphanoglu F, Farooq WA. Extraction of electronic parameters of organic diode fabricated with NIR absorbing functional manganese phthalocyanine organic semiconductor. *Synth Met*. 2011;161(15):1477-82.
6. Krasnov YS, Kolbasov GY, Tretyakova IN, Tomachynska LA, Chernii VY, Volkov SV. Dynamics of redox processes and electrochromism of films of zirconium (IV) phthalocyanines with out-of-plane β -dicarbonyl ligands. *Solid State Ion*. 2009;180(14):928-33.
7. de la Torre G, Vazquez P, Agullo-Lopez F, Torres T. Phthalocyanines and related compounds: organic targets for nonlinear optical applications. *J Mater Chem*. 1998;8(8):1671-83.
8. Basova TV, Hassan A, Durmus M, Gurek AG, Ahsen V. Orientation of the liquid crystalline nickel phthalocyanine films confined between electrodes. *Synth Met*. 2011;161(17-18):1996-2000.
9. Günsel A, Yarasir MN, Kandaz M, Koca A. Synthesis, H- or J-type aggregations, electrochemistry and in situ spectroelectrochemistry of metal ion sensing lead(II) phthalocyanines. *Polyhedron*. 2010;29(18):3394-404.
10. Komatsu T, Ohta K, Fujimoto T, Yamamoto I. Chromic Materials .1. Liquid-Crystalline Behavior and Electrochromism in Bis(octakis-N-Alkylphthalocyaninato)lutetium(III) Complexes. *J Mater Chem*. 1994;4(4):533-6.
11. Tillo A, Stolarska M, Kryjewski M, Popenda L, Sobotta L, Jurga S, vd. Phthalocyanines with bulky substituents at non-peripheral positions – Synthesis and physico-chemical properties. *Dyes Pigments*. 2016;127(Supplement C):110-5.

12. Sobotta L, Wierzchowski M, Mierzwicki M, Gdaniec Z, Mielcarek J, Persoons L, vd. Photochemical studies and nanomolar photodynamic activities of phthalocyanines functionalized with 1,4,7-trioxanonyl moieties at their non-peripheral positions. *J Inorg Biochem.* 2016;155:76–81.
13. Aydin M, Alici EH, Bilgili AT, Yarasir MN, Arabaci G. Synthesis, characterization, aggregation, fluorescence and antioxidant properties of bearing (4-(methylthio)phenylthio) tetra substituted phthalocyanines. *Inorganica Chim Acta.* 2017;464:1–10.
14. Benavente-Garcia O, Castillo J, Marin FR, Ortuno A, Del Rio JA. Uses and properties of Citrus flavonoids. *J Agric Food Chem.* 1997;45(12):4505–15.
15. Middleton E, Kandaswami C, Theoharides TC. The effects of plant flavonoids on mammalian cells: Implications for inflammation, heart disease, and cancer. *Pharmacol Rev.* 2000;52(4):673–751.
16. Olivati CA, Riul JA, Balogh DT, Oliveira JO, Ferreira M. Detection of phenolic compounds using impedance spectroscopy measurements. *Bioprocess Biosyst Eng.* 2009;32(1):41–6.
17. Usuda J, Kato H, Okunaka T, Furukawa K, Tsutsui H, Yamada K, vd. Photodynamic therapy (PDT) for lung cancers. *J Thorac Oncol.* 2006;1(5):489–93.
18. Bacellar IOL, Tsubone TM, Pavani C, Baptista MS. Photodynamic Efficiency: From Molecular Photochemistry to Cell Death. *Int J Mol Sci.* 2015;16(9):20523–59.
19. Qinglong B, Chunhua Z, Chuanhui C, Wancheng L, Jin W, Guotong D, Synthesis, Photophysical Properties and Near Infrared Electroluminescence of 1(4),8(11),15(18),22(25)-Tetra-(methoxyphenoxy)phthalocyanine. *Chinese Journal of Chemistry.* 2012;30:689–94.
20. Güzel E, Çetin Ş, Günsel A, Bilgiçli AT, Şişman İ, Yarasir MN. Comparative studies of photophysical and electrochemical properties of sulfur-containing substituted metal-free and metallophthalocyanines. *Res Chem Intermed.* :1–19.
21. Atmaca GY, Dizman C, Eren T, Erdogmus A. Novel axially carborane-cage substituted silicon phthalocyanine photosensitizer; synthesis, characterization and photophysicochemical properties. *Spectrochim Acta Part -Mol Biomol Spectrosc.* 2015;137:244–9.
22. Sen P, Atmaca GY, Erdogmus A, Dege N, Genc H, Atalay Y, vd. The Synthesis, Characterization, Crystal Structure and Photophysical Properties of a New Meso-BODIPY Substituted Phthalonitrile. *J Fluoresc.* 2015;25(5):1225–34.
23. Guzel E, Atmaca GY, Erdogmus A, Kocak MB. Novel sulfonated hydrophilic indium(III) and gallium(III) phthalocyanine photosensitizers: preparation and investigation of photophysicochemical properties. *J Coord Chem.* 2017;70(15):2659–70.
24. Yasa G, Erdogmus A, Ugur AL, Sener MK, Avciata U, Nyokong T. Photophysical and photochemical properties of novel phthalocyanines bearing non-peripherally substituted mercaptoquinoline moiety. *J Porphyr Phthalocyanines.* 2012;16(7–8):845–54.
25. Kirbac E, Atmaca GY, Erdogmus A. Novel highly soluble fluoro, chloro, bromo-phenoxy-phenoxy substituted zinc phthalocyanines; synthesis, characterization and photophysicochemical properties. *J Organomet Chem.* 2014;752:115–22.
26. Tayfuroglu O, Atmaca GY, Erdogmus A. Novel peripherally substituted zinc phthalocyanine: synthesis, characterization, investigation of photophysicochemical properties and theoretical study. *J Coord Chem.* 2017;70(18):3095–109.
27. Kobayashi N, Sasaki N, Higashi Y, Osa T. Regiospecific and Nonlinear Substituent Effects on the Electronic and Fluorescence-Spectra of Phthalocyanines. *Inorg Chem.* 1995;34(7):1636-.
28. Ozcesmeci I, Burat AK, Bayir ZA. Synthesis and photophysical properties of novel unsymmetrical metal-free and metallophthalocyanines. *J Organomet Chem.* 2014;750:125–31.
29. Durmus M, Ahsen V. Water-soluble cationic gallium(III) and indium(III) phthalocyanines for photodynamic therapy. *J. Inorganic Biochem.* 2010; 104: 297–309.